HYDROPLANING AVOIDANCE – A HOLISTIC SYSTEM APPROACH

Bernd Hartmann
Anton Klöster
Dr. Matthias Kretschmann
Dr. Thomas Raste
Continental AG
Germany
Paper Number 19-0256

ABSTRACT

Accidents in severe weather mainly arise due to a drastic loss of friction between the tires and the road surface unexpected by the driver. Beside all kinds of slippery winter conditions hydroplaning situations are even more dangerous not just for manually driven vehicles but also for automated vehicles when cruising at speeds above 80 to 100 km/h. This paper describes the Continental approach for a cascaded holistic safety system in imminent hydroplaning situations independent of the degree of automation. First, to reduce the overall hydroplaning risk a continuous tire tread depth monitoring function is integrated to trigger a timely replacement of worn-out tires. Second, a surround view camera and new tire-sensor-based early hydroplaning risk recognition allows an in-time driver warning or a system-initiated speed adaptation in case of automated vehicles. Especially for Automated Driving (AD) vehicles it is of major importance to avoid hydroplaning before it happens. Third, this information is send to the cloud-based eHorizon service so that also other traffic participants can be informed before entering a hydroplaning risk area. In case hydroplaning cannot be avoided a control system is designed and tested to evaluate an innovative assistance strategy in hydroplaning situations. The test cases demonstrate the suitability of this assistance concept.

1. INTRODUCTION

Heavy rain and bad weather conditions involving reduced traction because of wet, snowy and icy surfaces have been major contributory factors to traffic accidents in general. Extreme weather conditions are responsible for 39% of all accidents in Germany, [2]. One of the most dangerous driving situations is hydroplaning, which is difficult to predict and almost impossible to manage for the driver but also for automated vehicles. The hydroplaning situation depends on both vehicle and tire conditions as well as on environmental parameters such as water film thickness on the road. During hydroplane steering generally is not possible, because tire-road friction is completely lost at the front axle and therefore any transfer of lateral and longitudinal forces is not possible by the front tires anymore. Today's measures to avoid the risk of hydroplaning are almost exclusively infrastructure-based such as roadway draining and/or speed limits.
The Continental AG is developing a cross-divisional bundle of vehicle-based solutions proposing a cascaded holistic approach. This holistic approach is based on the four following cornerstones:

- Avoid
- Predict
- Warn
- Assist

Beside the proposal to analyze vehicle dynamics and controllability in hydroplaning situations and sketch an active safety system to assist the driver safely through this dangerous situation the main scope of this paper is to avoid the hydroplaning danger by a continuous tire tread depth monitoring system and the integration of two complimentary sensor-based systems to detect the imminent hydroplaning risk in an early pre-hydroplane phase before hydroplaning occurs. This information is used to warn the driver or to actively control the speed of an automated vehicle in imminent hydroplaning risk situations. Additionally, in such cases the potential risk to other vehicles on the road can be mitigated by an early communication via V2X technology and eHorizon, facilitating

a network of solidarity where one vehicle acts as a safety sensor for all other vehicles and not just those in its direct vicinity. eHorizon can provide this information to vehicles that could potentially be affected, so they are able to adjust their routing and driving functions to the risky weather conditions.

2. HYDROPLANING THEORY

A hydroplaning imminent situation can be explained by the following three-phase tire zone model concept in figure 1.

Exemplarily at a vehicle speed of 100 km/h a discrete element of the tire tread (P1) has a total contact duration with the surface and its top water layer of only 5 msec, where the three phases as displayed in the figure are passed through. In phase 1 the tread element is touching the water surface and displacing the water into the void volume of the tire's tread pattern. In phase 2, when the void is filled with water, the tire is analogously acting as a slick tire and more water cannot be absorbed by the void volume any more. This is the reason why the excessive water must be displaced to the front and to the sides underneath the tire.

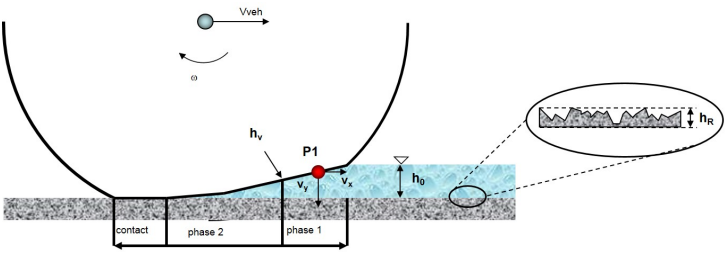

Figure 1. Three-Zone model concept for hydroplaning: separation zone (phase1), intermediate zone (phase2) and contact zone

As long as the tire's inside pressure is higher than the water pressure generated by the water wedge in front of the tire, the tire is successful in displacing the water to keep its road surface contact in the runout of the footprint. Just if the pressure relation changes and

the pressure of the water wedge in front gets higher than the tire's inside pressure the tire will swim up. This water displacement phase before it comes to hydroplaning is used to be detected by the systems for an early hydroplaning warning. This physics are the reason why there is a reasonable good chance to warn the driver up-front before the tires will completely hydroplane.

The critical vehicle speed is calculated as the averaged footprint length (L_m) divided by the touch down time (t_A) for a discrete tread element (P1), where the touch down time depends on the water height (h_0), the surface roughness (h_R) and the radius (R) for a circular tread bar, [1].

$$v_{krit} = \frac{L_m}{t_A} \qquad \text{(Equation 1)}$$

$$t_A = \frac{R/2}{2\sqrt{\frac{p_m}{\rho}}} \cdot \ln \frac{1+\sqrt{1-h_R/h_0}}{1-\sqrt{1-h_R/h_0}} \qquad \text{(Equation 2)}$$

With a mean support pressure (p_m) of 0,3 MPa, a density (ρ) for water of 1000 kg/m^3, a water height (h_0) of 8mm and a surface roughness (h_R) of 1mm the characteristic squeeze-out velocity for the water is approximately 35 m/sec. This results in considerably splash and spray water as a physical principal effect before it comes to hydroplaning. This splash water effect together with the oscillation caused by the water wedge in front of the tire's footprint is used by the system to detect the hydroplane risk in the pre-hydroplane phase.

3. TIRE TREAD DEPTH MONITORING

A critical factor in the context of hydroplaning is the residual tread depth of each tire. While periodic checks are sometimes done when changing from summer to winter tires (and back), there is no permanent monitoring of the tread depth. When using all season

tires, or in regions where the local climate does not require a seasonal change of the tires, the only tread depth monitoring relies on the user. Continental's TreadDepthMonitoring function continuously estimates the tread depth of each tire and can provide a timely recommendation for a tire change. Based on the tire mounted sensor eTIS (electronic Tire Information System) which was launched for the European tire pressure monitoring aftermarket in 2014, the system can now access not only the tire Pressure P and temperature T, but also the acceleration of the tire itself – not only the RIM. This allows for several new features (see also the direct indication of hydroplaning in chapter 5.2). It is clear, that by means of the tire acceleration, it is possible to measure the footprint length, which combined with the tire pressure provides the tire load L. Similarly, it is possible to accurately measure the impact factors influencing the dynamical tire radius R_{Dyn}. The dynamical tire radius itself can accurately be obtained by utilizing the wheel speed sensors ω in context with a GPS reference velocity V^{GPS} (see fig. 2) and state of the art methods dealing with the geometric impact of curves and situations that produce slip. Given that the tread of a tire is a rather slowly varying parameter, unsuitable situation (e.g. high tire slip) can be discarded and the remaining measurements can be filtered appropriately to deal with remaining measurement noise and effects like tire belt expansion in the beginning of a tire life.

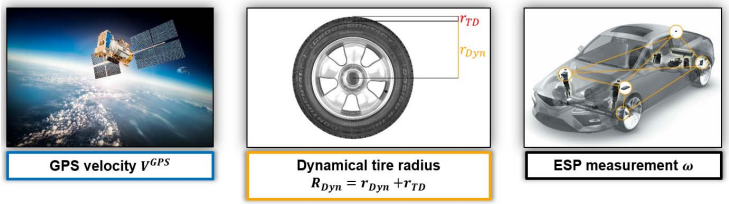

Figure 2. Dynamical tire radius R_{Dyn} separated into two contributions 1) Dynamical tire radius up to the tread r_{Dyn} and 2) Dynamical tire radius from tread r_{TD}

This accurately determined dynamical tire radius is impacted by the tire velocity V, tire pressure P, tire load L, tire temperature T and finally the tire tread depth r_{TD}.

$$V^{GPS} = R_{Dyn} \times \omega = [r_{Dyn}(P, T, V, L) + r_{TD}] \times \omega \quad \text{(Equation 3)}$$

Common to all the impact factors is that their impact depends on measurable noise factors. Here eTIS is an integral component for the tire pressure, load, and temperature, while the velocity V can be obtained from ω. After compensating for the noise factors and employing state of the art learning techniques to deal with manufacturing tolerances, the remaining impact on the tires dynamical radius is its tread depth which can be extracted by proper algorithms from r_{TD}. Based on this tread depth the following information (see figure 3) can be communicated to the driver in context with a specific tire type (e.g. summer vs. winter tire):

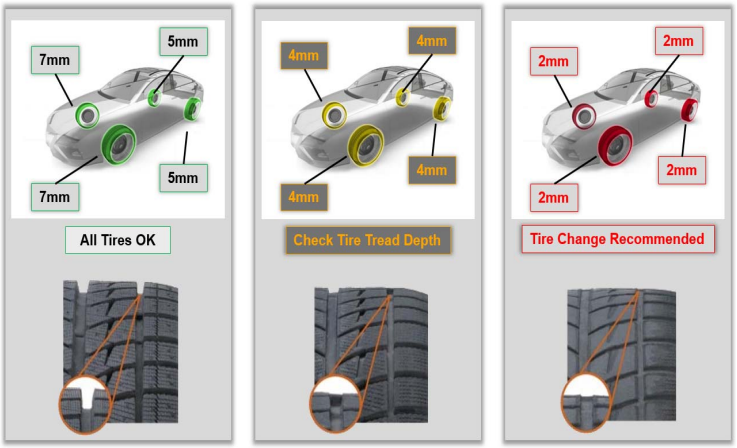

Figure 3. Information strategy for timely tire replacement

This provides ample time for an upcoming necessary tire replacement. Additionally, suboptimal tread depth levels (like the ones indicated in orange and red can be treated by the vehicle in context with the current velocity and information from the other

systems presented in this paper. This can then lead to a speed warning to the driver or a direct reduction of velocity via autonomous driving systems. In the following figure results are shown where the system was installed after some 8.000km into tires which were subsequently driven for another 40.000km on the front axle before they needed replacement, while the tires on the rear axle lasted a total of 60.000km. The vehicle has a front wheel drive architecture. The green lines indicate reference measurements together with min / max values (indicated by the bars). The black line is the output of the systems algorithm, while the red lines indicate the algorithms own error estimation. After carrying out several fleet campaigns with different vehicles and mission profiles, the overall accuracy of the algorithm was found to be +/-1mm, which is clearly achieved for the specific tire life on the vehicle in figure 3.

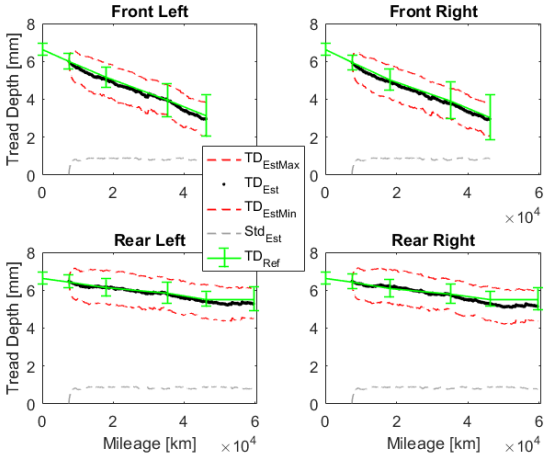

Figure 4. Results of TreadDepthMonitoring for the 4 tires of a front wheel drive vehicle driving a total of 60.000km

The front tires have been replaced after some 47.000km. The solid black line is the output of the algorithm with the red dashed lines being an error estimation. The green lines are reference measurements with corresponding uncertainties (bars).

4. LEVERAGING eHORIZON SERVICES

Weather has a strong impact on the road friction and thus the driver safety. For instance, after a long period without rain, a lot of particles and oils percolate through the road surface. Thus, at the beginning of rainfall, those oils ascend on the top of the road, resulting in a reduced friction potential.

Precisely predicting rainfall and especially friction related weather conditions is a major requirement for the future of Automated Driving solutions. This precision must not only boil down to temporal and spatial but to a strong reflection of the weather phenomena.

Nevertheless, forecasts delivered by the Weather Forecast Providers (WFP) are not sufficient in both spatial and temporal resolution. Actually, those forecasts might be sufficient at the city level (1 km square grid and hourly update) but not for Automated Driving (A.D.) and Advanced Driver Assistance Systems (A.D.A.S.) purposes: for which less than 100 meters of precision and below 5 minutes of frequency update are required. Figure 5 shows 4 weather cells near Frankfurt-City, WFP weather cell size is 1/100 of degree (in both longitude and latitude).

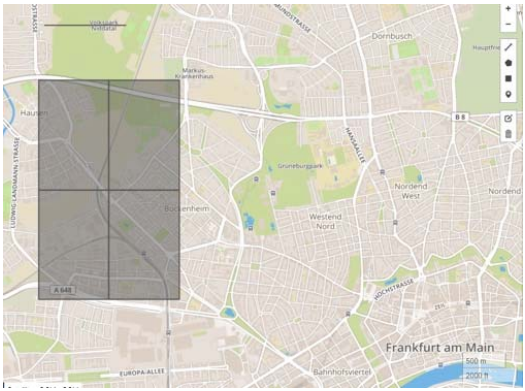

Figure 5. Example of weather cells in Frankfurt a. M.

Relying on vehicles as IoT weather stations, is a way to overcome this precision drawback. Vehicles are constantly collecting a large amount of weather related data and producing real-time weather-related observation system (*i.e.* activation of wiper, lights, and user or automated actuators as well as the information from temperature, hygrometry and pressure sensors). At a local level, vehicle data can be used to enhance weather forecast data. For instance, when a driver encounters a rainfall, either he activates the wipers, or the rain sensor is enabled. Those events are uploaded to the cloud where they are used to update short term weather forecasts. Wiper activation at the vehicle level increases the probability of precipitation at the cell level and thus each car contributes to changing the probability of the weather phenomenon. Figure 6 illustrates this behaviour. Thus, from local information, *eHorizon* produces a high accuracy map from both WFP and vehicle data.

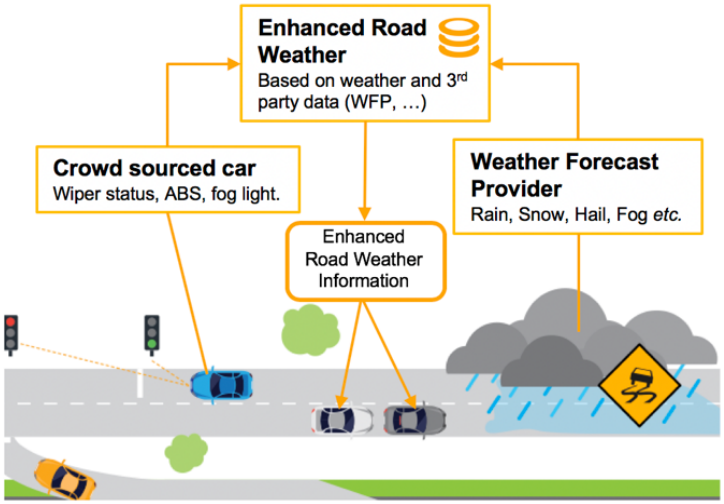

Figure 6. Road Weather Enhancement using vehicle data

The confusion matrix below compares results on rain detection for a Weather Forecast Provider (WPF) and our Road Weather (RW) service for a trip of 20 minutes with rain by only one vehicle. As the

matrix shows, the WFP does not predict rain for the whole trip (only 69%). RW, with only one vehicle, increases the precision by 30% (90% of good classifications).

Table 1.
Confusion Matrix for rain weather

	% False Predictions	% True Predictions
Rain : WFP	31%	69%
Rain : RW	10%	90%

With eHorizon Road Surface Condition services as an extension of eHorizon Road Weather it becomes possible to predict weather related situations and their impact on the road conditions and tire/road friction for the road ahead. Machine Learning approaches facilitate training of personalized road models to detect friction related hazardous weather situations such as hydroplaning or black ice. This method allows an accurate and fast prediction for a single road segment. eHorizon supports driving functions by delivering required information along the vehicle path in advance, before sensors can detect dangerous situations in immediate surroundings.

Adverse weather with heavy rain and exceptionally when first vehicles have already experienced and detected pre-hydroplane or even (full) hydroplane the information about the potential hydroplane risk for a specific weather cell is send to eHorizon. eHorizon services again will provide this information to other vehicles that could potentially be affected, so that they are able to adjust their driving functions to the risky weather conditions.

5. PREDICTIVE HYDROPLANING RISK RECOGNITION

5.1. Water Spray Recognition by surround view cameras

The approach to integrate surrounding sensors for early hydroplaning risk detection is because emerging of hydroplaning goes along with increasing water pressure between the tire's

footprint and the road surface which generates the above-mentioned splash water and spray in all directions (see chapter 2). The physical effect of the squeezed-out water is used to be detected and classified by an intelligent surround view camera system.

Figure 7. Water spray detected by surround view cameras for vehicle near field sensing

Surround view systems are based on four miniaturized wide-angle cameras, one front, one rear and two side cameras integrated in the base of the two exterior mirrors. These systems provide a 360° panorama view as well as single images from all four cameras in the near-field of the vehicle's environment. Additionally, to the sole imaging functionalities a bundle of different functionalities based on computer vision algorithms can be offered to the customer. Main use cases are parking functionalities with scalable level of automation.

The main goal of the surround view camera approach for this application is to use computer vision and machine learning methods to discriminate between different road conditions and to detect the imminent risk of hydroplaning. Figure 8 shows an example image of

the right-side mirror-integrated camera for the hydroplane risk recognition and the relevant region of interest (ROI) in red to be evaluated.

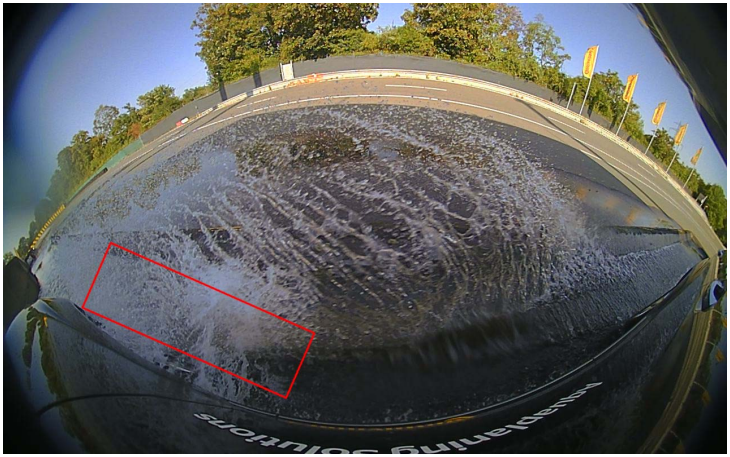

Figure 8. An example of the ROI for the Hydroplane (risk) class

To automatically distinguish between different road conditions, a classification framework based on Fisher Vector Encoding [14], which has become the state-of-the-art approach for a variety of image classification tasks, is proposed. In a pre-processing step, a Region Of Interest (ROI) is extracted from the original surround view image (see figure 9). The determination of its location, shape, and size is a crucial aspect for robust classification. On the one hand, the ROI must provide sufficient information to allow for the separation of the different classes. On the other hand, however, the ROI should only cover as few as possible information of the environment, since characteristics, which are not related to the actual road condition, might cause overfitting, especially in the case of limited training data. Once an appropriate ROI is defined, a compact and generic representation of the image is computed.

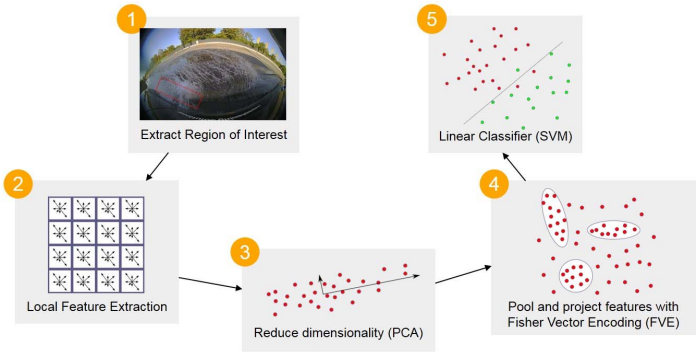

Figure 9. Typical pipeline for digital image processing

For this purpose, a set of local image features are extracted on a regular dense grid. For instance, the frequently used Histograms of Oriented Gradients (HOG) [12] feature descriptors can be applied to obtain a compact feature vector for each grid cell by computing a histogram of occurrences of image gradient orientations. In a further step, it is possible to reduce the dimensionality of the feature space by applying Principal Component Analysis (PCA) [13] and discarding the dimensions that contain the least information. Finally, the set of feature vectors are embedded into one global representation per image using Fisher Vector Encoding (FVE) [14]. In the training phase, a Gaussian mixture model is fitted to the training data. During encoding, the gradient of the log-likelihood with respect to the model parameters are determined based on the soft assignments of every local descriptor to each Gaussian distribution of the mixture model. Those gradients can be understood as adjustments to the parameters of the trained model with respect to a given image which results in a generic and unique representation. The gradients of individual model parameters are finally concatenated into a single global feature vector for each image. In the last step of the proposed framework, a classifier is trained to obtain a mapping from global feature vectors to road condition classes. As suggested by the authors of FVE [14], a linear Support Vector Machine (SVM) [15] is applied, where the feature

space is separated by a hyperplane which is determined during training. Thereby, the hyperplane is defined by a small set of training examples located at the class boundaries which are referred to as support vectors. Furthermore, a probabilistic output can be achieved by applying logistic regression.

The avoidance of overfitting poses a challenge in the particular case of hydroplane. Overfitting means the memorization of the training data, rather than understanding the concepts of the classes. As it is extremely dangerous to drive in hydroplaning situations in "real-world situations" on public roads the training data for this class can only be generated in a safe proving ground environment. The state-of-the-art test site of Continental is called "Contidrom". Here are different water basins for tire tests available that can be filled up to a specified water depth to create different reproducible hydroplaning situations in a safe vehicle test environment. So far there are no examples of hydroplaning from real world situations available for training. Therefore, special precautions must be taken to learn the typical characteristics of hydroplane. In this paper, the results of two different basic experiments are presented. For the experiment "only Contidrom", the system is trained and tested on images for all three classes (dry, wet & hydroplane risk) generated just at the safe proving ground environment. In the experiment "all Data" the system is trained and tested on images from the "Contidrom" proving ground (all three classes) as well as from "real-world situations" on public roads for dry and wet conditions only. Furthermore, hydroplaning situations only from the "Contidrom" are provided, as no real-world data can be generated safely for this class. In both experiments 50% of the data is used for training and the remaining 50% for testing, then the sets are switched in a second run.

Table 2 shows the first results of the experiments for both cases. The Overall Recognition Rate (ORR) describes the ratio of correct classifications to the number of samples, whereas Average Recognition Rate (ARR) calculates this ratio per class, averaged over classes. The "Contidrom" tests form the baseline for the experiments, as no real-world influences are present. Hydroplaning risk is detected correctly in 97.4% of the cases.

Table 2.
Results of the experiments: ORR (Overall Recognition Rate; ARR (Average Recognition Rate) per class

Experiment	ORR	ARR	Dry	Wet	Hydroplane
only „Contidrom“	95.6%	95.0%	93.3 %	94.4 %	**97.4%**
all Data	**98.5%**	**96.0%**	**99.0 %**	**100 %**	89.2%

The experiment “all Data” shows, that the system can learn the real-world situation well and even exceeds the “Contidrom” results for both ORR and ARR. However, a decreasing detection rate for hydroplaning is apparent in this setting. This suggests that the system has not only learned hydroplaning features but has also taken features of the test site environment into account. Since there is a much higher variability in the road characteristics for “real-world”, the classification of hydroplaning is a much more difficult task.
More experiments were carried out, where the system was only trained on “Contidrom” data and tested on a mixture of “Contidrom” and “real-world” data. In these settings, system performance decreased for wet and dry roads. This shows that the classifier trained only on the “Contidrom” data is prone to overfitting on the training environment and is not able to generalize very well.

Since no large data set of real-world hydroplaning data can be generated safely, potential overfitting on the test site environment has to be prevented in a different way. The biggest improvements can be achieved by generating more data for the case of hydroplaning by a wide variation of surrounding influences, e.g., different road surfaces, perturbations, and illumination situations. Additionally, methods of data augmentation to artificially generate more variability in the training data can be applied.

The first experiments clearly show that the discrimination between the different road conditions by surround view cameras is possible and on a good way. In particular, also the combination with feature

detection by a front camera and the enhancement by Deep Learning algorithms shows to be very promising.

5.2. Water Pressure Recognition by new Tire Sensors

Beside the usage of the eTIS Sensor for tire tread depth estimation, information about the interaction between the tire footprint region and the road when water is present is specifically of high interest. A model is outlined that explains a unique signature of hydroplaning in the radial acceleration that is measured by the sensors inbuilt accelerometer. The intended target is the detection of the very first manifestations of hydroplaning before the tire has lost a substantial amount of grip. Such an approach allows an early warning at vehicle speeds lower than the speed that ultimately results in full hydroplaning. With such an approach many of the driving situations that gradually lead to hydroplaning can be detected and by means of a driver warning or a more direct velocity reduction full hydroplaning can be avoided altogether.

For a constant water film covering a road, it is well known [11] that increasing the vehicle velocity when driving on a wet road causes the tire road interaction to change through different stages. At low velocities, where the water can fully be absorbed by the tire's void volume of the tread, the tire road interaction is characterized by its "normal" wet grip behavior. When increasing the velocity, at some point the tire's tread is not able any longer to fully absorb the water (ref. also Chapter 2). There will be a water wedge build-up in front of the tire, which partially penetrates underneath the forward-facing section of the footprint region, while the rest of the footprint region still has full & partly wet grip on the road. Consequently, the tire has lost only a fraction of its contact area and still enables vehicle control for most practical purposes. This state is of special interest for the detection with the eTIS sensor. When increasing the vehicle velocity even more, at some point the water wedge will fully penetrate between the footprint of the tire and the road. At this point, the tire has lost its contact to the road and there is no more grip at all. This state can be labelled as full hydroplaning.

5.2.1. Model for radial acceleration measured by eTIS

A model is presented explaining the radial accelerations seen by the eTIS sensor during the three different stages (wet grip, pre-hydroplaning, full hydroplaning). It explains how the concept introduced in Chapter 2 (ref. also Fig. 1) is sensed by the accelerometer in the eTIS Module.

In Fig. 10d) the radial acceleration a_R measured by eTIS as a function of the rotation angle ϕ is plotted. This acceleration data is based on an interpolation between different acceleration values derived from the corresponding curvature experienced on the path that eTIS moves along. Assuming that the longitudinal velocity V is constant along the circumference of the tire, the radial acceleration at a given rotation angle ϕ is given by,

$$a_R = V^2 / r(\phi) \qquad \text{(Equation 4)}$$

where $r(\phi)$ is the radius of the circle locally converging to the path of the eTIS. The left part (Figs. 8a and 8d) shows the case of wet grip. At 0° the radial acceleration is defined by the radius of curvature of the tire r_0, i.e. by V^2 / r_0. When the sensor enters the footprint region, the radius of curvature decreases to smaller values. The largest acceleration corresponds to the smallest radius r_1, i.e. V^2 / r_1. Inside the footprint area the path is nearly flat, i.e. the corresponding radius of curvature is very large which produces a measured acceleration of roughly 0. When leaving the footprint, the acceleration overshoot is approximately the same as when entering, i.e. V^2 / r_1. Finally, eTIS experiences the radial acceleration corresponding to the radius r_0, i.e. V^2 / r_0 at 360°.

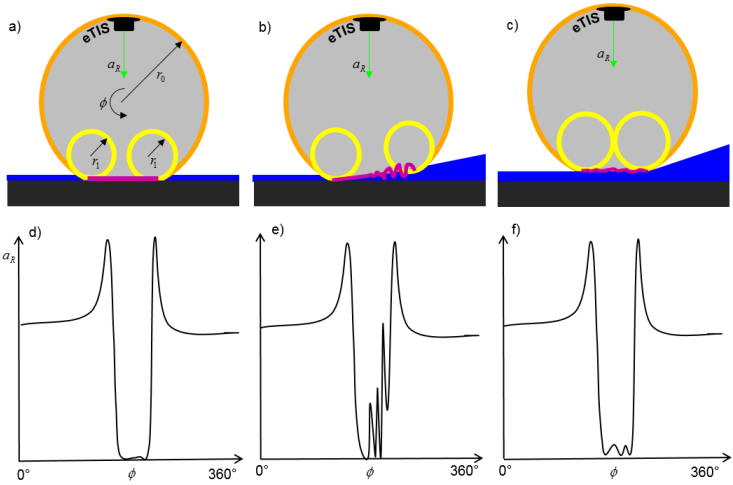

Figure 10. eTIS radial Acceleration as a function of the tire rotation angle. a), d): wet grip. b), e): pre-hydroplaning. c), f): full hydroplaning. a), b), c): Radius of curvature corresponding to top position (orange), entering/leaving the footprint (yellow), inside the footprint (magenta). d), e), f): Radial acceleration model output for eTIS position

In the case of pre-hydroplaning (Fig. 10b and 10e), this picture changes uniquely in the footprint region. Due to the penetration of the water wedge at the leading footprint edge, the small radius r_1 does not directly go to large values but shows oscillations during this transition phase. These oscillations originate from the expulsion of the water at the leading footprint edge. They are much less present at the trailing edge. Consequently, a unique asymmetry between trailing and leading edge in the case of pre-hydroplaning can be expected.

In the case of full hydroplaning (Fig. 10c and 10f) the tire slides virtually friction less over the water. In this case, the oscillations are expected to be of much smaller amplitude since the contact to the road is completely lost.

5.2.2. Hydroplaning tests with eTIS

To test the model, a vehicle was equipped with eTIS samples that specifically focus on measuring the radial acceleration around and in the footprint region. This vehicle has been driven on a test track into a water basin with approximately 10-20 mm of water. The vehicle was fitted with new "Continental Viking Contact 205/55R16" tires with full tread depth. In a first test run the vehicle was driven with 60km/h over a wet road. In this case, the shape of the measurement resembles the expectation for the wet grip case (Fig. 10d).
In a second test run attention towards the radial acceleration when driving with 60km/h inside the water basin was payed, where the full hydroplaning threshold was ~75km/h. This pre-hydroplaning situation was analyzed in the time domain and also by means of a spectrogram in the following figure:

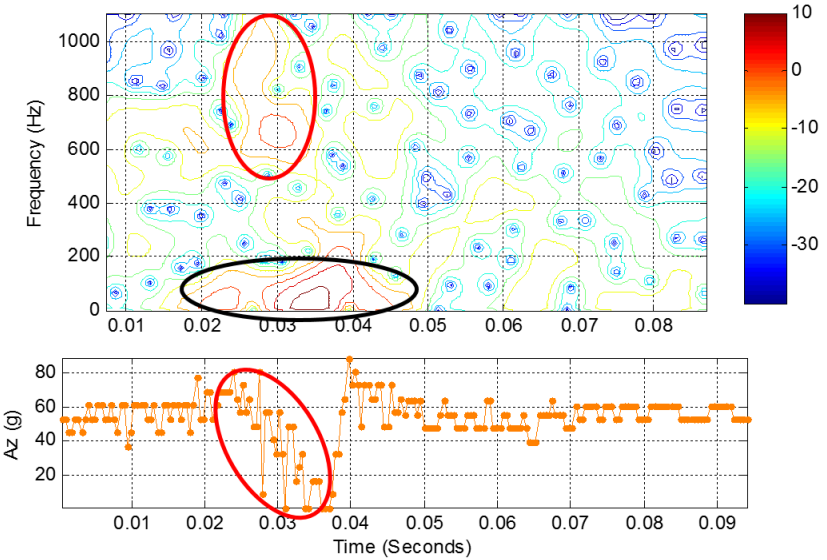

Figure 11. eTIS radial acceleration and spectral density

At the bottom of the figure, the eTIS radial acceleration signal as a function of time for this typical pre-hydroplaning situation is

plotted. It is important to note that when plotting against the time, the leading edge occurs before the trailing edge. In Fig. 10, the acceleration curve was plotted as a function of the counterclockwise defined rotation angle ϕ. The leading edge displayed exactly the oscillations expected from the expulsion of the water (red diagonal oval). These oscillations are not visible at the trailing edge. Consequently, the expected strong asymmetry was fully visible in the time-domain.

At the top of the figure, the spectral density (color coded) as a function of the same time axis and also the frequency (y-axis) is displayed. One can clearly see an increased spectral density of rather low frequencies (0…200Hz) that is distributed somewhat symmetrically over the entire footprint area (indicated by a black oval). Additionally, an increased spectral density is also clearly visible at higher frequencies (500-1100Hz), but only around the leading edge (indicated by red oval). This analysis reveals an asymmetry between the leading and the trailing edge of the footprint. The spectrogram confirms the higher frequency oscillations associated with the leading edge of the footprint, visible on the time signal, while also evaluating quantitatively the frequency range of the oscillations - roughly 500 Hz to 1100 Hz.

Theory and measurements show promising potential for the detection of pre-hydroplaning. A unique asymmetric signature in the radial acceleration measurement has been identified. The corresponding eTIS based detection is able to trigger the prevention of full hydroplaning.

6. HYDROPLANING ASSISTANCE BY BRAKE INTERVENTION AT THE REAR AXLE

6.1. Active Safety Assistance

In a hydroplaning situation the driver needs assistance in two distinct ways: firstly, to stabilize the vehicle in case of disturbances and secondly, to guide the vehicle safely along the course of the road. For control design a linear single-track model is used, in which

the front tire forces are neglected due to the hydroplaning behavior. The state vector **x** contains yaw rate and side slip angle as state variables. Control input **u** is the rear axle longitudinal force difference. This control action can be provided e.g. by torque vectoring based on rear wheel individual braking. The disturbance input **s** is an unknown yaw torque M_z. caused e.g. by not homogeneous water film thickness at the front left and right wheels.

The assistance is triggered by evaluating wheel slip and other signals provided by a standard ESC (Electronic Stability Control) system. The controller is designed as a state feedback in combination with feed-forward of the driver steering input **w** and disturbance compensation, i.e. the control law is given by

$$\boldsymbol{u = -K_x x - K_s \hat{x}_s + K_w w} \qquad \text{(Equation 5)}$$

The control structure is further extended by an inner-loop longitudinal slip control described in [4] to access the full control potential whilst ensuring that the rear axle will not be destabilized during the intervention. The sign of the control variable **u** determines which rear wheel is in slip control mode. The overall control structure of the hydroplaning active safety assistance is shown in Figure 12. Details of the design of the controller are given in [3].

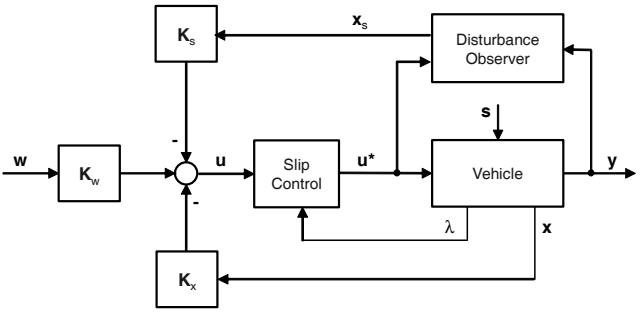

Figure 12. Control structure of the hydroplaning active safety assistance system with inner-loop slip control and outer-loop yaw rate control

6.2. Vehicle test results

Figure 13 illustrates the hydroplaning tests with a rear-drive vehicle at the “Contidrom” proving ground. The hydroplaning basin is 100 m long and 6 m wide. The water film thickness is approx..10 – 20 mm.

Figure 13. Hydroplaning assistance vehicle test at the “Contidrom” proving ground with front wheels floating. The vehicle is controllable by rear wheel brake torque vectoring

The following figure illustrates the assistance principal as well as typical vehicle dynamics signals.

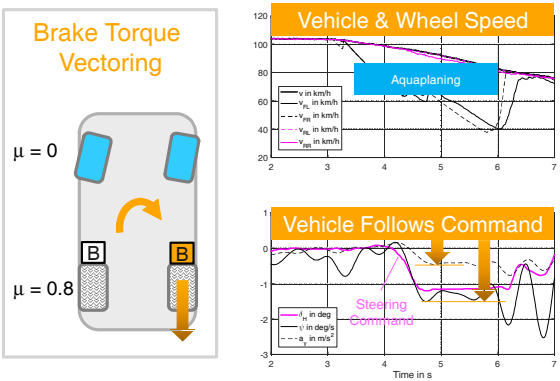

Figure 14. Hydroplaning vehicle tests at the “Contidrom” proving ground. (Left): Assistance principle: vehicle is controllable by torque vectoring at the rear axle. (Right):

Vehicle dynamics showing that vehicle is following driver steering command during hydroplaning phase

Figure 14 illustrates the performance of the hydroplaning assistance. The driver initiated a steering wheel angle ramp-step during floating phase of the front wheels. With the assistance system active the vehicle is controllable and follows the driver commands by building up sufficient yaw rate and lateral acceleration. Without assistance the vehicle is moving uncontrollable in straight direction despite driver steering command.

7. CONCLUSIONS

The integration of the eTIS-based TreadDepthMonitoring function is intended to avoid driving with too low tire tread depth during heavy rain and adverse weather situations in the first place. A surround view camera and tire sensor (eTIS) based system for early hydroplaning risk detection has been proposed to recognize the imminent hydroplane risk and to warn the driver or to intervene in the case for an automated vehicle in an early phase before (full) hydroplaning occurs. Based on outdoor vehicle tests in real hydroplaning situations feasibility studies have been carried out where both systems demonstrate the potential and ability for a proof of concept and further base development.
After adverse weather and pre-hydroplane events have been detected the cloud-based eHorizon services will be updated and provides services to inform other vehicles that could be affected before entering the hydroplane risk area.
Further-on a simulation environment has been designed to study an active safety system with the purpose to assist within the physical limits when the vehicle already hydroplanes (full). An extended tire model reproduces the effect of the surface water leading to a complete loss of grip at the front wheels. The proposed assistance strategy is based on a state feedback and feed-forward control torque vectoring actuating the rear brakes. The system enables an adequate amount of yaw damping as well as a minimum guidance capability. Vehicle tests have shown significant benefit of the assistance.

The hydroplaning assistance as proposed in this paper is the next

step to strongly support Continental's long-term strategy "Vision Zero" leading to zero traffic-related fatalities, injuries and road accidents in future.

8. References

1] Bathelt, H.: Analytische Behandlung der Strömung in der Aufstandsfläche schnell rollender Reifen auf nasser Fahrbahn ("Aquaplaning"). *PhD Thesis*, *Technische Hochschule,* Wien, 1971.

[2] Ditze, M.; Golatowski, F.; Laum, N.; Varhelyi, A.; Gustafsson, S.; Geramani, K.: A Survey on Intelligent Vehicle Safety Systems for Adverse Weather Conditions. In, *Proc. of FISITA World Automotive Congress*, Budapest, 2010.

[3] Frerichs, D.: Design and Simulation of Vehicle Dynamics Control to Improve Stability during Aquaplaning. *Master Thesis, Technical University,* Darmstadt (in German), 2015.

[4] Gengenbach, W.: The Behavior of Passenger Car Tires on Dry and Wet Roads. *PhD Thesis, Technical University,* Karlsruhe (in German), 1967.

[5] Görich, H.-J.: System That Detects the Current Friction Potential of a Passenger Car During Driving. *PhD Thesis*, VDI-Verlag, Düsseldorf (in German), 1993.

[6] Herrmann, S.R.: Simulation Model of Water Drainage and Aquaplaning on Road Surfaces. *PhD Thesis,* Stuttgart (in German), 2008.

[7] Müller, P.C. & Lückel, J.: Disturbance Rejection Control in Linear Multivariable Systems. In *Regelungstechnik,* Heft 2, pp. 54-59 (in German), 1977.

[8] Orend, R.: Modelling and Control of a Vehicle with Single-Wheel Chassis Actuators. In *Proc. of IFAC World Congress*, Prague, 2005.

[9] Raste, T., Frerichs, D.: Study on Active Safety for Aquaplaning Assistance. In *Proc. of AVEC International Symposium*, Munich, 2016.

[10] Semmler, S., Isermann, R.; Schwarz, R.; Rieth, P.: Wheel Slip Control for Antilock Braking Systems Using Brake-By-Wire Actuators. In *Proc. of SAE World Congress*, Detroit, 2002.

[11] Tuononen A., Niskanen A., Xiong Y., Mahboob-Kanafi M.: Advanced Tire Sensing for wet grip and rolling resistance improvements. *Intelligent Tire Technology,* 2013

[12] Dalal, N. and Triggs, B.: Histograms of Oriented Gradients for Human Detection, In: IEEE Computer Society Conference on Computer Vision and Pattern Recognition, 2005

[13] Pearson, K. F.R.S.: On lines and planes of closest fit to systems of points in space, In: The London, Edinburgh, and Dublin Philosophical Magazine and Journal of Science, Pages 559-572, 1901

[14] Sánchez J., Perronnin, F., Mensink T., Verbeek, J.: Image Classification with the Fisher Vector: Theory and Practice, In: International Journal of Computer Vision Vol 105 Issue 3, Pages 222-245, December 2013

[15] Cortes, C. Vapnik, V.: Support-Vector Networks, In: Machine Learning, Pages 273-297, 1995